

# Impact of Side Branches on the Computation of Fractional Flow in Intracranial Arterial Stenosis Using the Computational Fluid Dynamics Method

Liu, H., Lan, L., Leng, X., Ip, H. L., Leung, T. W. H., Wang, D. & Wong, K. S.

Author post-print (accepted) deposited by Coventry University's Repository

**Original citation & hyperlink:**

Liu, H, Lan, L, Leng, X, Ip, HL, Leung, TWH, Wang, D & Wong, KS 2017, 'Impact of Side Branches on the Computation of Fractional Flow in Intracranial Arterial Stenosis Using the Computational Fluid Dynamics Method', Journal of Stroke and Cerebrovascular Diseases, vol. 27, no. 1, pp. 44-52.

<https://dx.doi.org/10.1016/j.jstrokecerebrovasdis.2017.02.032>

DOI 10.1016/j.jstrokecerebrovasdis.2017.02.032

ISSN 1052-3057

ESSN 1532-8511

Publisher: Elsevier

**NOTICE: this is the author's version of a work that was accepted for publication in Journal of Stroke and Cerebrovascular Diseases. Changes resulting from the publishing process, such as peer review, editing, corrections, structural formatting, and other quality control mechanisms may not be reflected in this document. Changes may have been made to this work since it was submitted for publication. A definitive version was subsequently published in Journal of Stroke and Cerebrovascular Diseases, 27, (2017)**

**DOI: 10.1016/j.jstrokecerebrovasdis.2017.02.032**

© 2017, Elsevier. Licensed under the Creative Commons Attribution-NonCommercial-NoDerivatives 4.0 International <http://creativecommons.org/licenses/by-nc-nd/4.0/>

Copyright © and Moral Rights are retained by the author(s) and/ or other copyright owners. A copy can be downloaded for personal non-commercial research or study, without prior permission or charge. This item cannot be reproduced or quoted extensively from without first obtaining permission in writing from the copyright holder(s). The content must not be changed in any way or sold commercially in any format or medium without the formal permission of the copyright holders.

**This document is the author's post-print version, incorporating any revisions agreed during the peer-review process. Some differences between the published version and this version may remain and you are advised to consult the published version if you wish to cite from it.**

**Impact of side branches on computation of fractional flow in intracranial arterial stenosis using computational fluid dynamics method**

Haipeng Liu<sup>1,2#</sup>, Linfang Lan<sup>1#</sup>, Xinyi Leng<sup>1</sup>, Hing Lung Ip<sup>1</sup>, Thomas WH Leung<sup>1</sup>,  
Defeng Wang<sup>2\*</sup>, Ka Sing Wong<sup>1\*\*</sup>

<sup>#</sup>The two authors contributed equally to the work

<sup>\*</sup>Two corresponding authors

<sup>\*\*</sup> Corresponding author (clinical): Ka Sing Wong, Division of Neurology, Department of Medicine and Therapeutics, The Chinese University of Hong Kong, Prince of Wales Hospital, Hong Kong, China. Email:ks-wong@cuhk.edu.hk

<sup>\*</sup> Corresponding author (technical): Defeng Wang, Department of Imaging and Interventional Radiology, The Chinese University of Hong Kong, Shatin, Hong Kong SAR. Email:dfwang@cuhk.edu.hk, Tel: 852-26322975

<sup>1</sup> Division of Neurology, Department of Medicine and Therapeutics, The Chinese University of Hong Kong, Prince of Wales Hospital, Hong Kong, China.

<sup>2</sup> Research Center for Medical Image Computing, Department of Diagnostic and Interventional Radiology, The Chinese University of Hong Kong, Prince of Wales Hospital, Hong Kong, China.

## **Abstract**

**Background:** Computational fluid dynamics (CFD) allows noninvasive computation of fractional flow (FF) in intracranial arterial stenosis. Removal of small branches in cerebral arteries is necessary in CFD simulation. The impact of this simplification on the measurement of FF needs to be judged.

**Methods:** Idealized vascular model was built with 70% focal luminal stenosis. A branch with  $1/3$  or  $1/2$  radius of parent vessel was added at distance of 5, 10, 15 and 20 mm to the lesion, respectively. CFD was computed with assumptions of rigid vessel wall, blood as Newtonian fluid, incorporating pressure at inlet boundary, and flow rate at outlet boundary. Assignment of flow rate at bifurcation followed Murray's law. Five intracranial arteries reconstructed from patient-specific imaging were used to test the impact of simplification by including or removing side branches. Then a transient simulation was performed on a patient-specific model, with larger branch (branch/MCA radius ratio 0.63) for validation. Relative difference of FF within 5% range between paired models (branches included and removed) was considered as no impact on FF assessment.

**Results:** Compared with control model without branch, the relative differences of FF in models with side branches of  $1/3$  or  $1/2$  radius of parent vessels located at different distance to the stenosis, were less than 2%.

In five pairs of cerebral arteries (branches included and removed), FF were 0.876/0.877, 0.853/0.858, 0.874/0.869 0.865/0.858 and 0.952/0.948 respectively. The relative difference in each pair was less than 1%. In transient model, the relative difference of FF in a pair of models with or without branch was 3.5%.

**Conclusion:** The impact of removing side branches with radius < 50% of parent vessel on the accuracy of FF measurement in ICAS is negligible in static CFD simulation, and minor in transient CFD simulation.

**Key words:** Side branches, Fractional flow, Intracranial arterial stenosis, Computational fluid dynamics

## **Background**

Intracranial artery stenosis (ICAS) is a major cause for ischemic stroke and transient ischemic attack (TIA) with its etiology still not well known.[1, 2] Impaired hemodynamics related to the stenosis is considered an important mechanism for the ischemic event[3, 4]. In recent years, as a novel concept, fractional flow (FF) has been put forward to substitute the measurement of lumen diameter restriction which could not accurately evaluate the the risk of stroke because of the inconsideration of complex hemodynamic effects.[5] It was defined as ratio of maximal blood flow in the presence of stenosis to the blood flow in the normal artery, and can be approximately calculated as the ratio of the pressures in the areas posterior and anterior to the stenosis, as in the calculation of fractional flow reserve (FFR), which has been developed as a gold standard to reflect the hemodynamic significance of vascular stenosis in cardiovascular field.[6, 7] With the advantage of delineating lesion-specific ischemia, FFR has been used to guide the selection of patients for percutaneous coronary intervention.[8] In cerebrovascular field, a few pilot studies also showed that FF may be a useful predictor for recurrent stroke in patients with symptomatic ICAS.[9, 10] The analysis of specific influencing factors on cerebral FF, a promising parameter to reflect the hemodynamic significance of ICAS, is therefore significant.

Computational Fluid Dynamics (CFD), based on vascular geometry derived from clinical imaging, provides a new method for non-invasive assessment of FF.[8] [11]

[12] However, non-invasive FF is far from mature in gauging severity and treating of ICAS. As a relatively new concept in the field of ICAS, FF needs further researches into the details to validate its clinical implications. Thus, simplified models with acceptable accuracy are appropriate in the current stage. But the extent of simplification need to be judged. And the modeling process also calls for simplification. To perform CFD simulation, 3D vascular geometry is required, together with the properties of blood and vessel wall, and the inlet and outlet boundary conditions. In practical cerebrovascular simulation, due to limited ability of current imaging technique to accurately and fully delineate small vessels, it is inevitable to trim off some small branches. Since a side branch diverts blood flow from its parent artery with local flow pattern influenced, the removal may cause hemodynamic changes in the parent arteries. Especially, the pressure and thus FF value may be effected. Hence, reasonability of removing the side branches during CFD modeling should be judged.

## **Methods**

In CFD modeling, the radius of branches needed to be trimmed off are usually less than half of the radius of parent vessel. To study branching effect, we built ideal models of identical stenosis, with the location and radius of the branch varying among different models. By comparing the pressure and FF derived from CFD in different models (with and without branch), the effect of branching on FF can be investigated, relative difference more than 5% was deemed as significant.

## **1. Idealized models of vascular stenosis**

The idealized 3D model of vessel with stenosis was created as a long cylinder with radius of 1.5 mm, having a focal stenosis with 70% area reduction (Fig.1). Sufficient elongations were sustained before and after the stenosis (25 mm and 50 mm, respectively) to include the regions that might be affected by turbulence. A branch with 1/3 or 1/2 radius of parent vessel was added at distance of 5, 10, 15 and 20 mm posterior to the lesion, respectively, to generate different models. Hence, one reference model without branch and 8 models with branches of different radius and distance to the stenosis were studied using the CFD method.

## **2. CFD modeling of idealized vascular models**

Computation of mesh, simulation of blood flow and evaluation of hemodynamic characteristics of the arterial models, were performed using the ANSYS software package (ANSYS, Inc.). Mesh was created in all models with maximum element size 0.25mm globally and 0.1mm at inlet and outlet. The settings and assumptions for simulation of blood flow were as follows: Blood was an incompressible Newtonian fluid with a constant viscosity of  $0.004 \text{ kg}\cdot\text{m}^{-1}\cdot\text{s}^{-1}$  and a density of  $1060 \text{ kg}/\text{m}^3$ . The vessel wall was rigid, non-compliant wall with no-slip assumption. A total pressure of 110 mmHg was applied at the inlet and a flow rate was applied at the outlet(s). Mass flow rate at the outlet was calculated by the following formula: flow rate = mean velocity $\times$ outlet area $\times$ density. Mean velocity was set as 35cm/s, which is the typical mean flow velocity of cerebral arteries. Flow rate at the outlet of branches was



determined by Murray's law.[13] Thus, the total inlet flow rate would be added by the branch. From the reference model, control models for 1/3 and 1/2 radius groups were made. As in the reference model, there were no branches in control models. However, the flow rates of control models for 1/3 and 1/2 branching groups, were respectively set identical to other models within the same group (increased according the size of branches). The simulation of blood flow was fulfilled by solving the Navier–Stokes equations. The convergence criterion for the relative residual of all dependent variables was set as  $10^{-4}$ .

Evaluation of hemodynamic characteristics was performed on pressure field of the models. As shown in Fig.1, section-averaged pressure was measured at proximal and distal to the stenosis. FF, which by definition is the flow rate of stenosed and normal flow rates, was simplified and calculated as the ratio of post- and pre-stenotic pressures. The relative difference of FF between the model with/without branch was defined as follows:  $(FF \text{ with branch} - FF \text{ in control model}) / FF \text{ in control model}$ .

### **3. Static CFD modeling of intracranial arteries**

To validate the results from idealized models, five intracranial arteries reconstructed from patient-specific imaging were used to test the impact of simplification by including and removing side branches. All the imaging data were obtained from a retrospective-prospective cohort study conducted in Prince of Wales Hospital, for which the protocol has been approved by the joint Chinese University of Hong Kong-New Territories East Cluster Clinical Research Ethic committee, Hong Kong.

Physiologically, the internal carotid artery (ICA), which branches into middle carotid artery(MCA) and anterior cerebral artery(ACA), is a main source of cerebral blood supply. 3D geometry of intracranial arteries containing MCA stenosis and small branches were extracted from CTA (Computed tomography angiography) source images using Mimics 18.0 (Materialise). The arterial segments start from supraclinoid ICA, and end at proximal MCA-M2 and distal ACA-A1. Side branches from MCA-M1 with radius  $<1/2$  of the parent vessels will be selected as the target branches, and be kept or removed during the simulation. Computation of mesh, simulation of blood flow and evaluation of hemodynamic characteristics of the arterial models were almost the same as in idealized models, except that the mean velocity of MCA and ACA at outlet were set as 35cm/s and 31cm/s based on the revised in-vivo measurement, respectively.[14]

#### **4. Transient CFD modeling of intracranial arteries**

All simulations above were static and based on given flow rate. To evaluate the effect of branching on FF under physiological conditions, transient simulations were performed on a patient-specific model (with a luminal 70% stenosis at MCA) and its counterpart without branch, as shown in Fig.2. Here the branch is large enough (with branch/MCA radius ratio 0.63) to take possible large branching effects into consideration. The blood pressure derived from in-vivo measurement was applied at ICA inlet.[15] Flow resistance is the ratio of pressure drop and flow rate:  $R = \Delta P/Q$ . In the distant flow resistance applied at an arterial outlet,  $\Delta P$  was the difference

between area-averaged outlet pressure and reference pressure  $P_0$ (5mm). The MCA and ACA distant flow resistances of 5.97 and 8.48 (unit:  $10^{-9}$  Pa.s.m<sup>-3</sup> ) which were commonly used values, were applied instead of any given flow rates to make the simulations more similar with physiological reality[16]. The branch/MCA distant flow resistance ratio was about 1/4, derived from their cross-section area ratio according to Murray's law. To get fully developed flow, inlet and outlets were lofted and elongated. To eliminate the initial transient effect, the simulations were performed in 3 cardiac cycles (0.8s each), with time step 0.005s. Transient values of flow rate, pressure and FF were compared between the two models.

## **Results**

### **1. Pressure distribution in idealized models**

Fig 3. shows the pressure derived from CFD simulation in idealized models with&without side branches. In all idealized models, pressure was fairly constant in the sections proximal and distal to the stenosis, while sharply dropped at and around the stenosis position. In idealized models with branches of 1/3 radius of parent vessels, the pressure (pre/post to stenosis) was 14405/12908,14405/12875,14405/12884 and 14405/12882 pa when side branches located at distances of 5, 10, 15 and 20 mm to the lesion, respectively. In control model with identical flow rate, the result was 14408/12853pa. In idealized models with branches of 1/2 radius of parent vessels, the pressure was 14366/12769, 14366/12755, 14366/12743 and 14366/12713 pa at different distances. The value of control model was 14365/12615pa.

## **2. FF in idealized models**

In idealized models with branches of 1/3 radius of parent vessels, the FF were 0.896, 0.894, 0.894 and 0.894 when side branches located at distances of 5, 10, 15 and 20 mm to the lesion, respectively (Fig.4). With identical total mass flow rate and other boundary conditions, the FF in control model (branch removed, but flow rate identical with branch-added models in the same group) was 0.892. Compared with control model, the relative differences of FF in models with side branches of 1/3 of parent vessels were all less than 1%.

In idealized models with branches of 1/2 radius of parent vessels, the FF were 0.889, 0.888, 0.887, 0.885 when side branches located at distances of 5, 10, 15 and 20 mm to the lesion, respectively (Fig.4). The FF in control model was 0.878. Compared with control model, the relative differences of FF in models with side branches of 1/2 parent-vessel radius were about 1%.

## **3. Static CFD modeling of intracranial arteries**

To precisely test the impact of side branches, CFD simulation was performed on five pairs of MCA models based on clinical imaging, with side branches included/removed. In five pairs of cerebral arteries (branches included/removed), FF were 0.876/0.877, 0.853/0.858, 0.874/0.869 0.865/0.858 and 0.952/0.948, respectively. Within each pair, the relative difference of FF was less than 1%.

## **4. Transient CFD modeling of intracranial arteries**

Fig.5 was derived from the results of second cardiac cycle to avoid any initial transient effects. As shown in the upper row, the branch effect on flow rate is only obvious in ICA(overall flow rate), with ACA and MCA nearly not effected. As to pressure, observable differences exists only at MCA. In the model with branch, the pressure curve of branch is nearly identical with, and overlapped on the MCA pressure curve. The similarity of their pressure was due to the positional approximation of MCA/branch outlets.

To further investigate global pressure distribution, the diastolic and systolic wall pressure distribution was shown in Fig.6. The distribution pattern was similar between models. From the scales, it can be derived that the branch effect is negligible on maximum pressure, but observable on minimum pressure (lower in model with branch, relative difference: 4.3% in diastolic and 5.9% in systolic). Since the minimum pressure area lies posterior to the stenosis of MCA, the FF value may be effected and need to be calculated.

Fig.7 shows the transient FF values of the two models, which were measured around the stenotic section, during the whole simulation. As estimated above, in the model with branch, the FF values are lower, corresponding to its relative low pressure value in post-stenotic area where minimum pressure lies. Time-averaged FF values in models with and without branch are 0.906 and 0.938, respectively, with relative difference 3.5%. Therefore, eliminating a branch with radius 63% of its parent

vessel's caused changes in the flow rate, and lower pressure distribution, but the relative error of FF was still small.

## **Discussion**

In this study, we investigated the impact of side branches on the accuracy of FF measurement by comparing between idealized vascular models with branches included/removed, and validated the results in imaging-based intracranial arteries. Compared with respective control models, the relative difference of FF within either group of models with branches of 1/3 or 1/2 radius of parent vessels, ranged below 1%. The CFD simulation of real intracranial arteries also showed FF changes less than 1% between models with branches included/removed. In the transient model, in which a branch with radius larger than 1/2 of parent vessel's was considered, the time-averaged FF change enhanced to 3.5%, still within 5% which was defined as significant difference. The enhancement of FF change can be attributed to two main factors. Firstly, for fully validation, a larger branch was simulated. The larger branch deviated more blood flow with more obvious effect on flow field. Secondly, in transient model there was dissipation caused by oscillation, which effected pressure distribution. These results collectively suggested that the removal of side branches with radius  $< 50\%$  of parent vessel may have little impact on the accuracy of FF measurement in ICAS.

Based on patient-specific vascular geometry, CFD permits non-invasive assessment of hemodynamics in cerebral arteries. The small branches are difficult to be entirely and

accurately pictured with current imaging technologies. Therefore, simplification of the vessel geometry is routinely performed before CFD simulation. However, removal of the side branches will probably affect flow field distribution and therefore lead to inaccuracy in pressure measurement. Prior study investigating the impact of side-branches on the flow simulation in coronary arteries implied that in coronary arteries the variation of volume flow caused by side branches would be up to 78.7% in the trunk.[17] The wall shear stress was consequently affected. These differences of hemodynamic characteristics caused by side-branches make it necessary to justify the reasonability of removing side branches during FF measurement using CFD method. What's more, as to ICAS, the application of FF is a relative new concept far from validated and mature. Thus, the measurement on the effects of simplification is very essential. For more solid validation of our conclusions here, and the application of CFD simulation of FF in intracranial arterial stenosis as a whole, further studies based on enough in-vivo data are necessary.

The pressure distribution in the current study showed that the pressure mainly dropped in situ of the stenosis, and was fairly constant in regions distal to the stenosis, even in the regions with branches, as shown in Fig.3. In ideal models with branches, the pressure distal to the stenosis slightly increased, compared with the control models without branches, but the relative differences were within 1%. This may be due to the shunting effect of branching on post-stenosis pressure field that released the energy dissipation caused by turbulence. The current results also showed that the location of

branches had little impact on the distal pressure. Therefore, the measurement position of distal pressure was reasonable.

The pressure drop mentioned above accords with theoretical computation from the hemodynamic view. The pressure drop caused by stenosis consists of three items of the flow rate: a linear item, a quadratic item and a transient item.[18] It has been applied in cerebrovascular hemodynamics.[19, 20] By neglecting the transient item, the formulation can be derived as  $\Delta P = A \cdot Q + B \cdot Q^2$ , where  $\Delta P$  means pressure drop and  $Q$  is the volume flow rate. The linear and quadratic terms show the energy loss caused by viscosity and turbulence respectively. Under current flow rate, in calculation we found the quadratic item was trivial compared with the linear item. So finally pressure drop is approximately proportional to the flow rate. According to Murray's Law, the flow rates in downstream branches from an identical parent vessel, are proportional to the cube of their radii. Here the flow rate in the main branch was kept a constant, therefore, the flow rate ratio of the three situations (without branch, with branch of 1/2 parent vessel radius, with branch of 1/3 parent vessel radius) is  $1:(1+1/27):(1+1/8)=216:224:243$ , the pressure drops and consequent FFs will be approximately equal, which conforms with our simulation results.

Simplified simulation conditions were necessary and appropriate. Firstly, solid vessel wall was applied in all models. The ideal model and five clinical models were based on the conditions of steady flow. These assumptions are commonly used in hemodynamic simulations. Parallel studies also showed the limited effect of solid wall



assumption.[21, 22] These simplifications were therefore reasonable. Secondly, the blood in its essence is non-Newtonian due to the shear-thinning effect. Here the choice for Newtonian fluid was based on the following three facts. 1) Our study was based on steady-state flow, but the difference caused by non-Newtonian effect is only prominent in transient simulation.[23] 2), Even in the transient models for pulsatile blood flow, the non-Newtonian effect on pressure is limited.[24] 3) What's more, the non-Newtonian models such as Casson models, are not better than Newtonian model in high shear rate areas.[25] Therefore, the Newtonian model is an appropriate choice for the current work.

The CFD modeling in current study have some limitations. Firstly, the boundary conditions limited the precision. Especially in transient model, the distal flow resistances and inlet ICA flow rate were derived from literature. This limitation may deviate simulation results from real patient-specific values. Therefore, the object of transient model was mainly for validation of the conclusions made under steady-flow conditions. This limitation can be solved by further study with in-vivo measurements. Secondly, in imaging-based intracranial arteries, downstream pressure was measured nearby the stenosis, where residual turbulence around the stenosis may still cause some minor perturbation on pressure field. Thirdly as a preliminary exploration in this field, only the effect of a single branch was investigated here, and the results showed little impact from removing branches with radius  $< 50\%$  of parent vessel. However, in the modeling of complex cerebral vessels with multiple branches, the interactions and total effects of branches need to be further studied.

## **Conclusion**

For CFD simulation of intracranial arteries, removal of side branches with radius < 50% of parent vessel has little impact on the accuracy of FF measurement in static CFD modeling, but may have minor impact in the transient CFD modeling. In cerebral vessel modeling, the simplification of vascular geometry is reasonable in CFD computation for the pressure field.

## **Acknowledgement**

The work described in this paper was partially supported by the General Research Fund (reference No. 14117414), Research Grant Council of Hong Kong, a grant from the Innovation and Technology Commission (Project No: GHP/028/14SZ) and a grant from Technology and Business Development Fund (TBF) (Project No: TBF15MED004).

## **Reference**

- [1] Chimowitz MI, Lynn MJ, Derdeyn CP, Turan TN, Fiorella D, Lane BF, et al. Stenting versus aggressive medical therapy for intracranial arterial stenosis. *New England Journal of Medicine*. 2011;365:993-1003.
- [2] Kim BJ, Kim JS. Ischemic stroke subtype classification: an Asian viewpoint. *Journal of stroke*. 2014;16:8-17.
- [3] Kwon H-M, Lynn MJ, Turan TN, Derdeyn CP, Fiorella D, Lane BF, et al. Frequency, Risk Factors, and Outcome of Coexistent Small Vessel Disease and Intracranial Arterial Stenosis: Results From the Stenting and Aggressive Medical Management for Preventing Recurrent Stroke in Intracranial Stenosis (SAMMPRIS) Trial. *JAMA neurology*. 2016:1-8.
- [4] Kim BJ, Kim SM, Kang DW, Kwon SU, Suh DC, Kim JS. Vascular tortuosity may be related to intracranial artery atherosclerosis. *International Journal of Stroke*. 2015;10:1081-6.
- [5] Liebeskind DS, Feldmann E. Fractional flow in cerebrovascular disorders. *Interventional neurology*. 2013;1:87-99.
- [6] Ullah M, Majumder A. Fractional Flow Reserve-A Review. *Cardiovascular Journal*. 2013;5:190-200.

- [7] Nakazato R, Park H-B, Berman DS, Gransar H, Koo B-K, Erglis A, et al. Noninvasive fractional flow reserve derived from computed tomography angiography for coronary lesions of intermediate stenosis severity results from the DeFACTO study. *Circulation: Cardiovascular Imaging*. 2013;6:881-9.
- [8] Koo B-K, Erglis A, Doh J-H, Daniels DV, Jegere S, Kim H-S, et al. Diagnosis of ischemia-causing coronary stenoses by noninvasive fractional flow reserve computed from coronary computed tomographic angiograms: results from the prospective multicenter DISCOVER-FLOW (Diagnosis of Ischemia-Causing Stenoses Obtained Via Noninvasive Fractional Flow Reserve) study. *Journal of the American College of Cardiology*. 2011;58:1989-97.
- [9] Leng X, Scalzo F, Ip HL, Johnson M, Fong AK, Fan FS, et al. Computational fluid dynamics modeling of symptomatic intracranial atherosclerosis may predict risk of stroke recurrence. *PloS one*. 2014;9:e97531.
- [10] Liebeskind DS, Kosinski AS, Lynn MJ, Scalzo F, Fong AK, Fariborz P, et al. Noninvasive fractional flow on MRA predicts stroke risk of intracranial stenosis. *Journal of Neuroimaging*. 2015;25:87-91.
- [11] Nørgaard BL, Gaur S, Leipsic J, Ito H, Miyoshi T, Park S-J, et al. Influence of coronary calcification on the diagnostic performance of CT angiography derived FFR in coronary artery disease: a substudy of the NXT trial. *JACC: Cardiovascular Imaging*. 2015;8:1045-55.
- [12] Liebeskind DS, Fong AK, Scalzo F, Lynn MJ, Derdeyn CP, Fiorella DJ, et al. SAMMPRIS angiography discloses hemodynamic effects of intracranial stenosis: computational fluid dynamics of fractional flow. *Stroke*. 2013;44:A156-A.
- [13] Nixon AM, Gunel M, Sumpio BE. The critical role of hemodynamics in the development of cerebral vascular disease: a review. *Journal of neurosurgery*. 2010;112:1240-53.
- [14] Moore S, David T, Chase J, Arnold J, Fink J. 3D models of blood flow in the cerebral vasculature. *Journal of biomechanics*. 2006;39:1454-63.
- [15] Sarrami-Foroushani A, Esfahany MN, Moghaddam AN, Rad HS, Firouznia K, Shakiba M, et al. Velocity measurement in carotid artery: Quantitative comparison of time-resolved 3D phase-contrast MRI and image-based computational fluid dynamics. *Iranian Journal of Radiology*. 2015;12.
- [16] Alastruey J, Parker K, Peiró J, Byrd S, Sherwin S. Modelling the circle of Willis to assess the effects of anatomical variations and occlusions on cerebral flows. *Journal of biomechanics*. 2007;40:1794-805.
- [17] Wellnhofer E, Osman J, Kertzscher U, Affeld K, Fleck E, Goubergrits L. Flow simulation studies in coronary arteries—impact of side-branches. *Atherosclerosis*. 2010;213:475-81.
- [18] Young DF, Tsai FY. Flow characteristics in models of arterial stenoses—II. Unsteady flow. *Journal of biomechanics*. 1973;6:547-59.
- [19] Karunanithi K, Han C, Lee C-J, Shi W, Duan L, Qian Y. Identification of a hemodynamic parameter for assessing treatment outcome of EDAS in Moyamoya disease. *Journal of biomechanics*. 2015;48:304-9.
- [20] Liang F, Fukasaku K, Liu H, Takagi S. A computational model study of the influence of the anatomy of the circle of Willis on cerebral hyperperfusion following carotid artery surgery. *Biomedical engineering online*. 2011;10:1.
- [21] Politis A, Stavropoulos G, Christolis M, Panagopoulos P, Vlachos N, Markatos N. Numerical modelling of simulated blood flow in idealized composite arterial coronary grafts: Transient flow. *Journal of biomechanics*. 2008;41:25-39.
- [22] Loth F, Fischer PF, Bassiouny HS. Blood flow in end-to-side anastomoses\*. *Annu Rev Fluid Mech*. 2008;40:367-93.

- [23] Campo-Deaño L, Oliveira MS, Pinho FT. A review of computational hemodynamics in middle cerebral aneurysms and rheological models for blood flow. *Applied Mechanics Reviews*. 2015;67:030801.
- [24] Amornsamankul S, Wiwatanapataphee B, Wu YH, Lenbury Y. Effect of non-newtonian behaviour of blood on pulsatile flows in stenotic arteries. *Int J Biol Med Sci*. 2006;1:42-6.
- [25] Fan Y, Jiang W, Zou Y, Li J, Chen J, Deng X. Numerical simulation of pulsatile non-Newtonian flow in the carotid artery bifurcation. *Acta Mechanica Sinica*. 2009;25:249-55.

Figure 1. Ideal models. First row: the reference model without branch and its side view. 2nd to 5th rows: models with branch of 1/3(left column) and 1/2(right column) main vessel radius located 5mm, 10mm, 15mm and 20mm from stenosis center.

Figure 2. Clinical models with branch reserved (upper) and eliminated (lower) and corresponding transient simulation conditions.

Figure 3. The pressure distribution 1: idealized model without branch. 2: idealized model with branch of 1/2 radius of parent vessel. 3: clinical model without branch. 4: clinical model with branch.

Figure 4. Fractional flow in models with branch located at different distances from the stenosis in ideal models. The data points at vertical axis indicated the control models (without branch, but flow rate identical with those models in the same group).

Figure 5. The flow rate and pressure at inlet(ICA) and outlets(ACA,MCA and branch) in two models within the second cardiac cycle.

Figure 6. Diastolic and systolic pressure distribution in the two models.

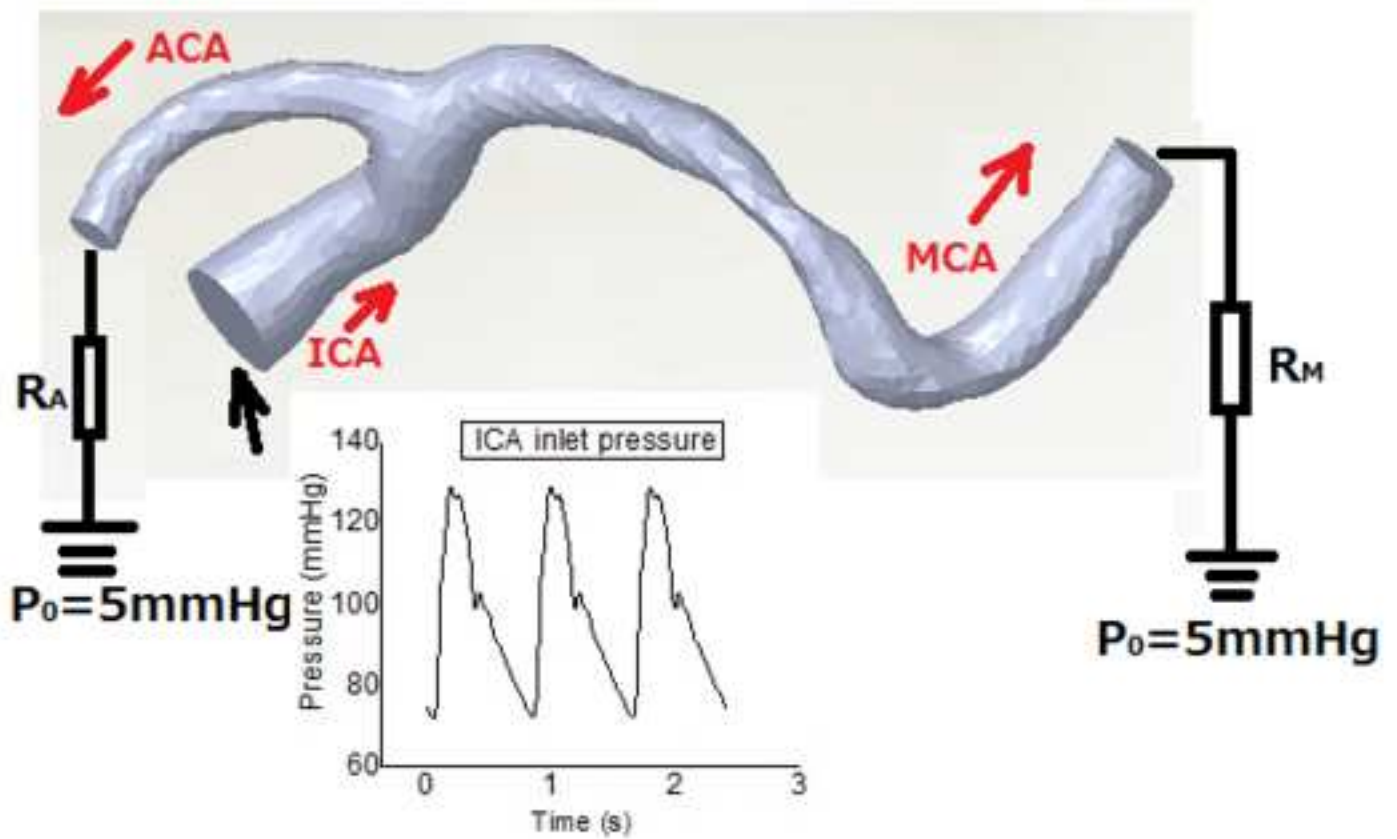
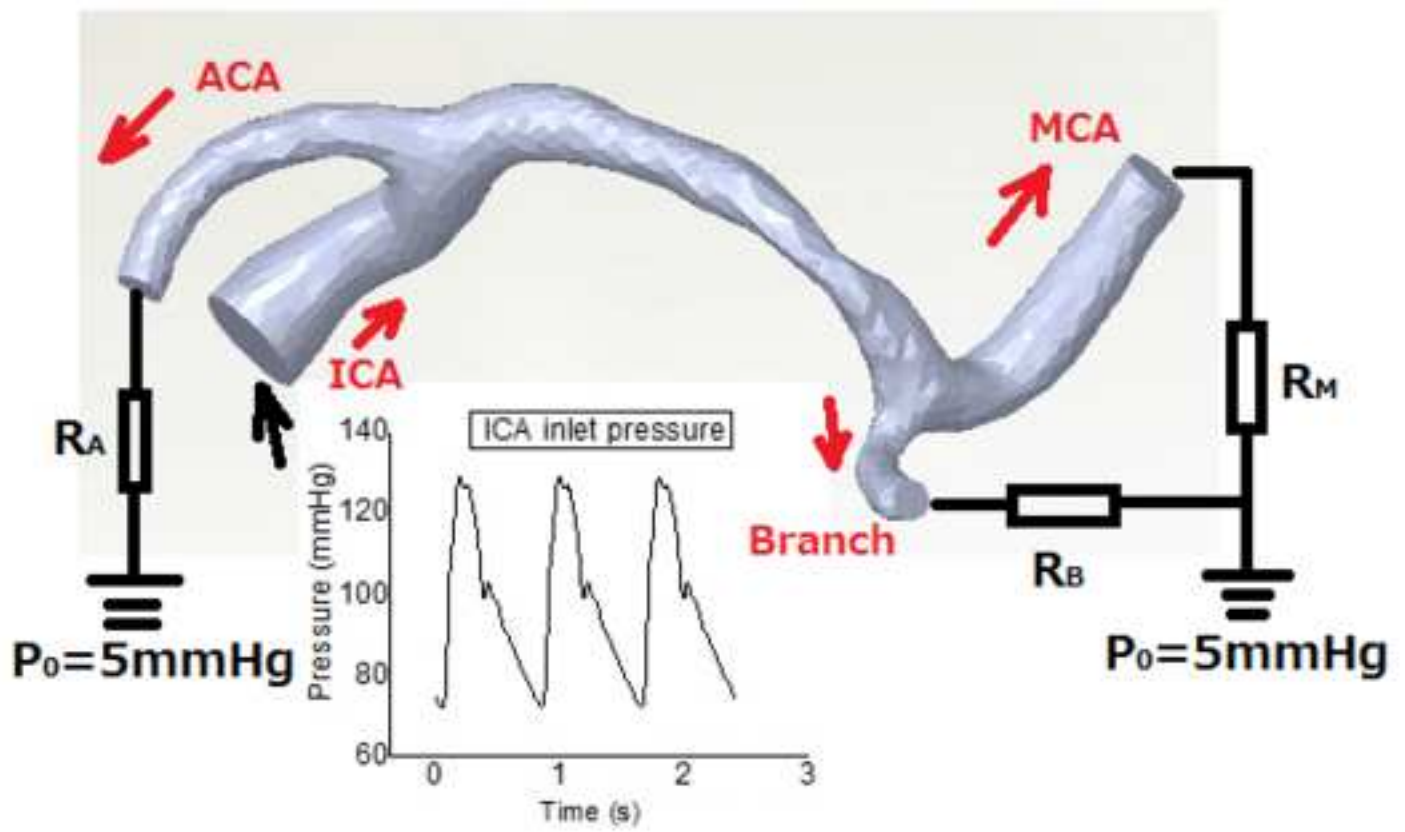
Figure 7. The measurement positions and transient FF values in the two models.

Figure(s)

[Click here to download high resolution image](#)

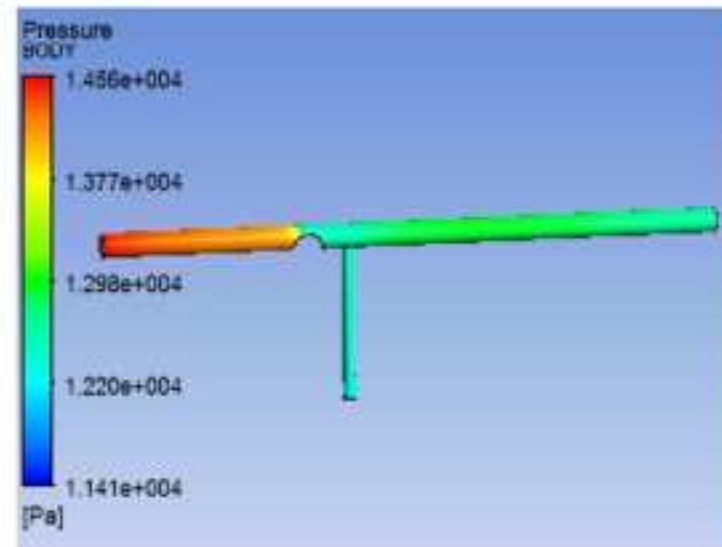
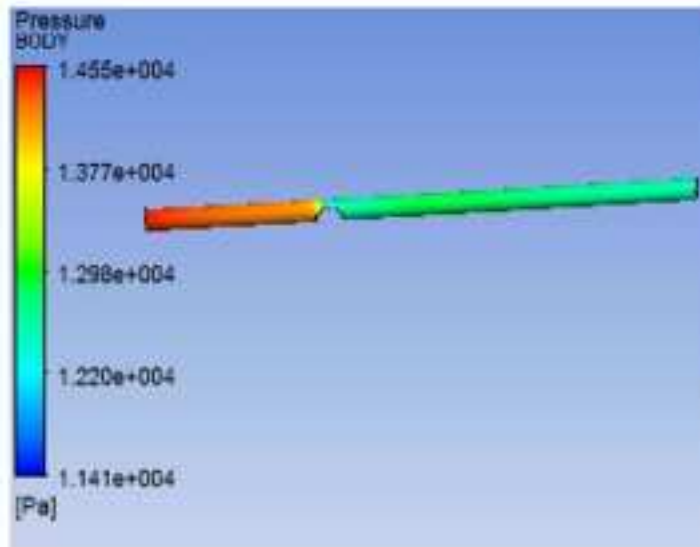


Figure(s)  
[Click here to download high resolution image](#)

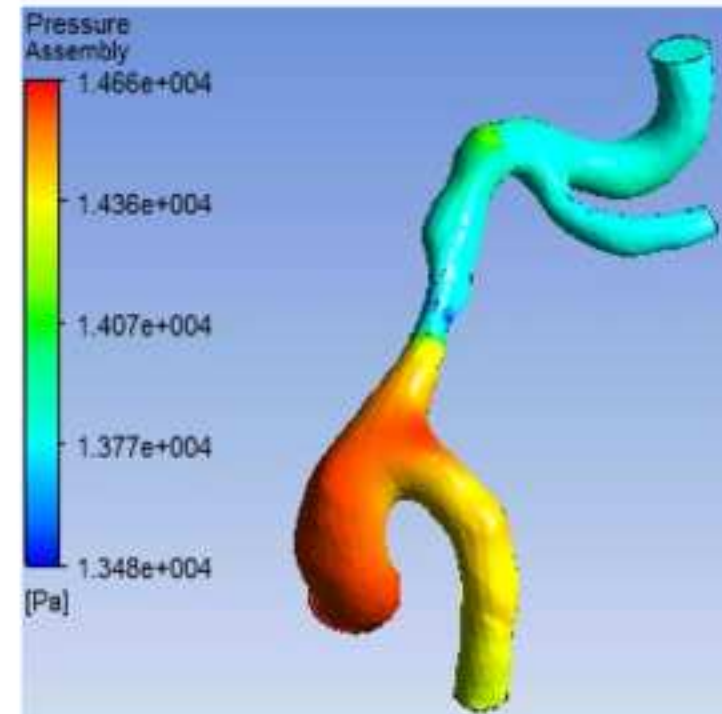
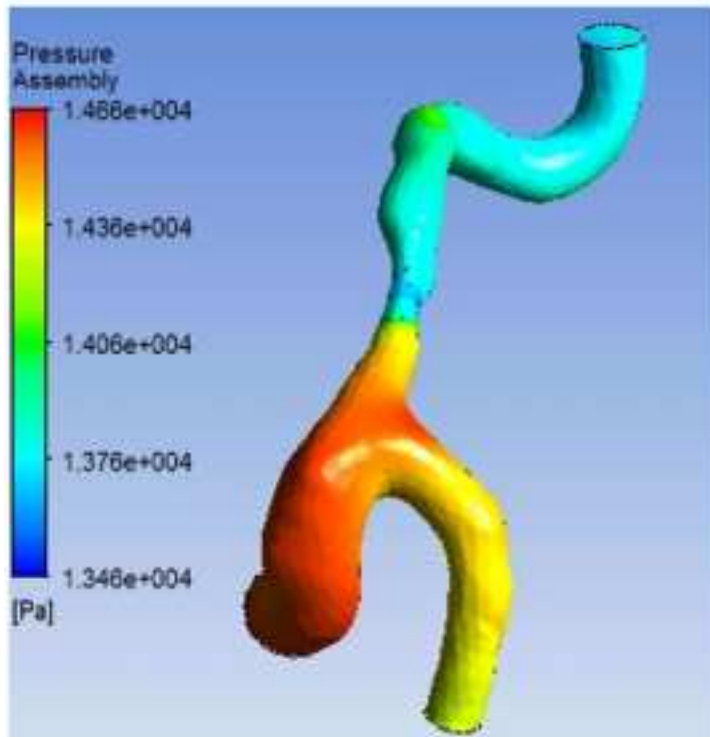


Figure(s)

[Click here to download high resolution image](#)



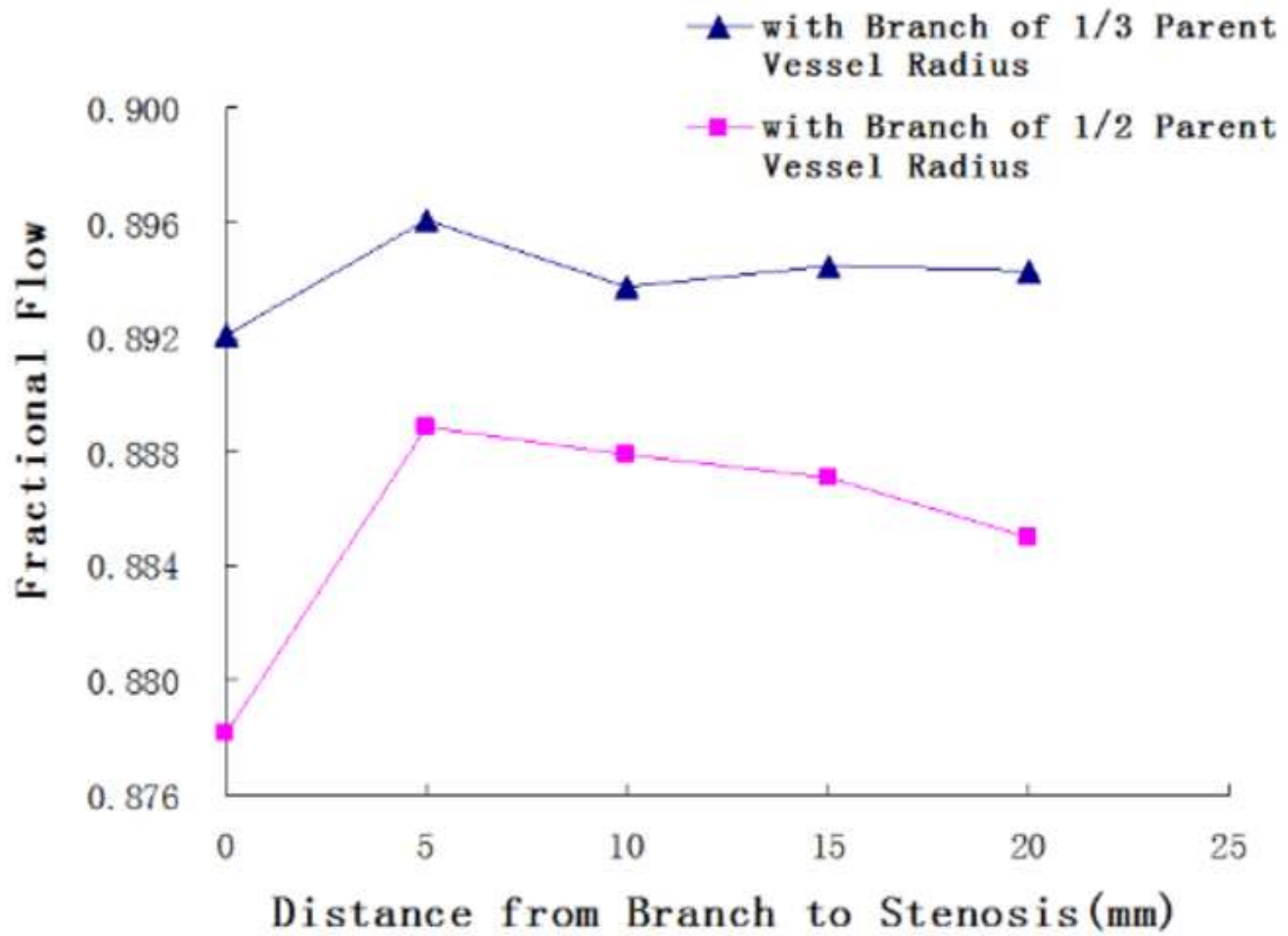
1	2
3	4



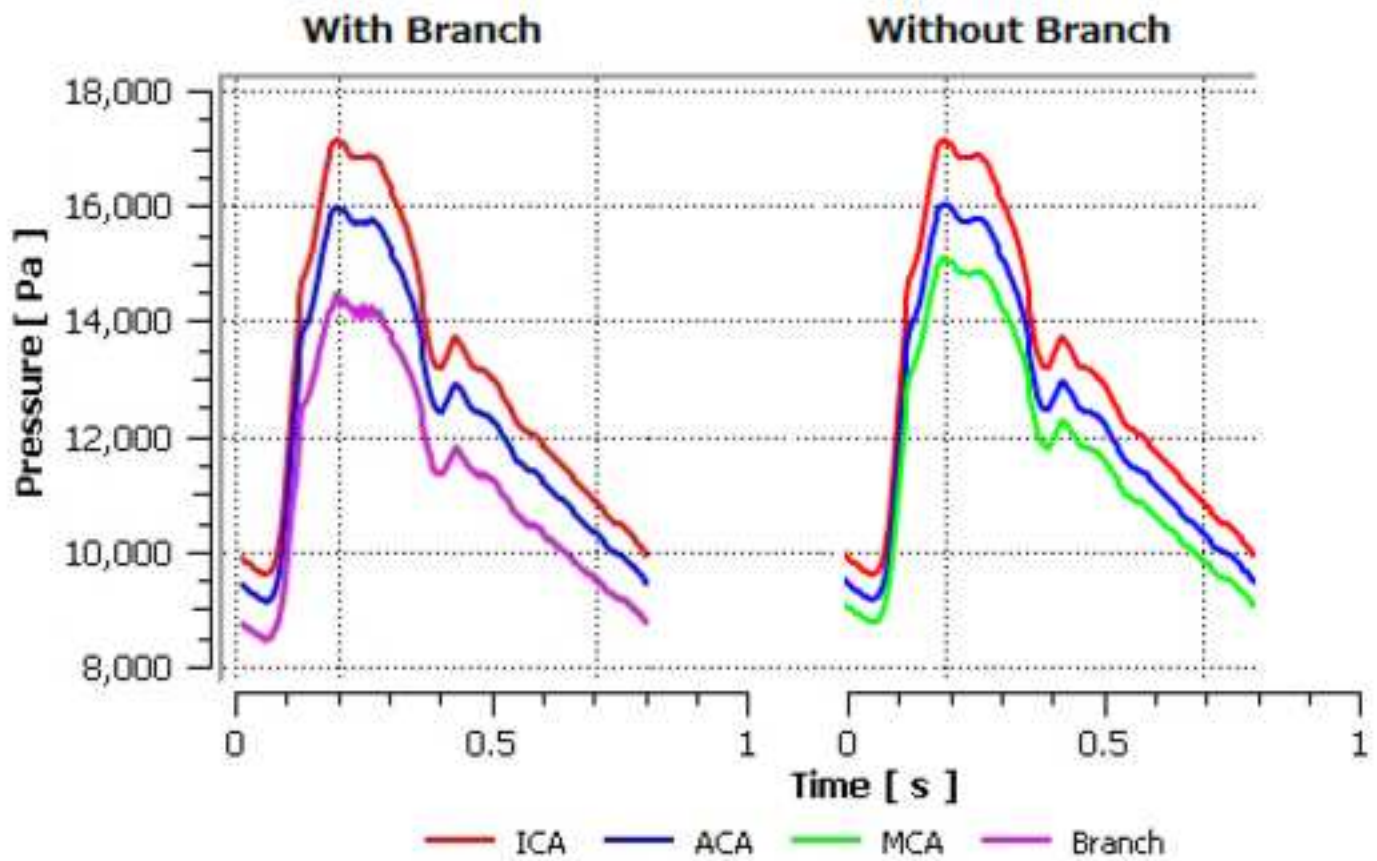
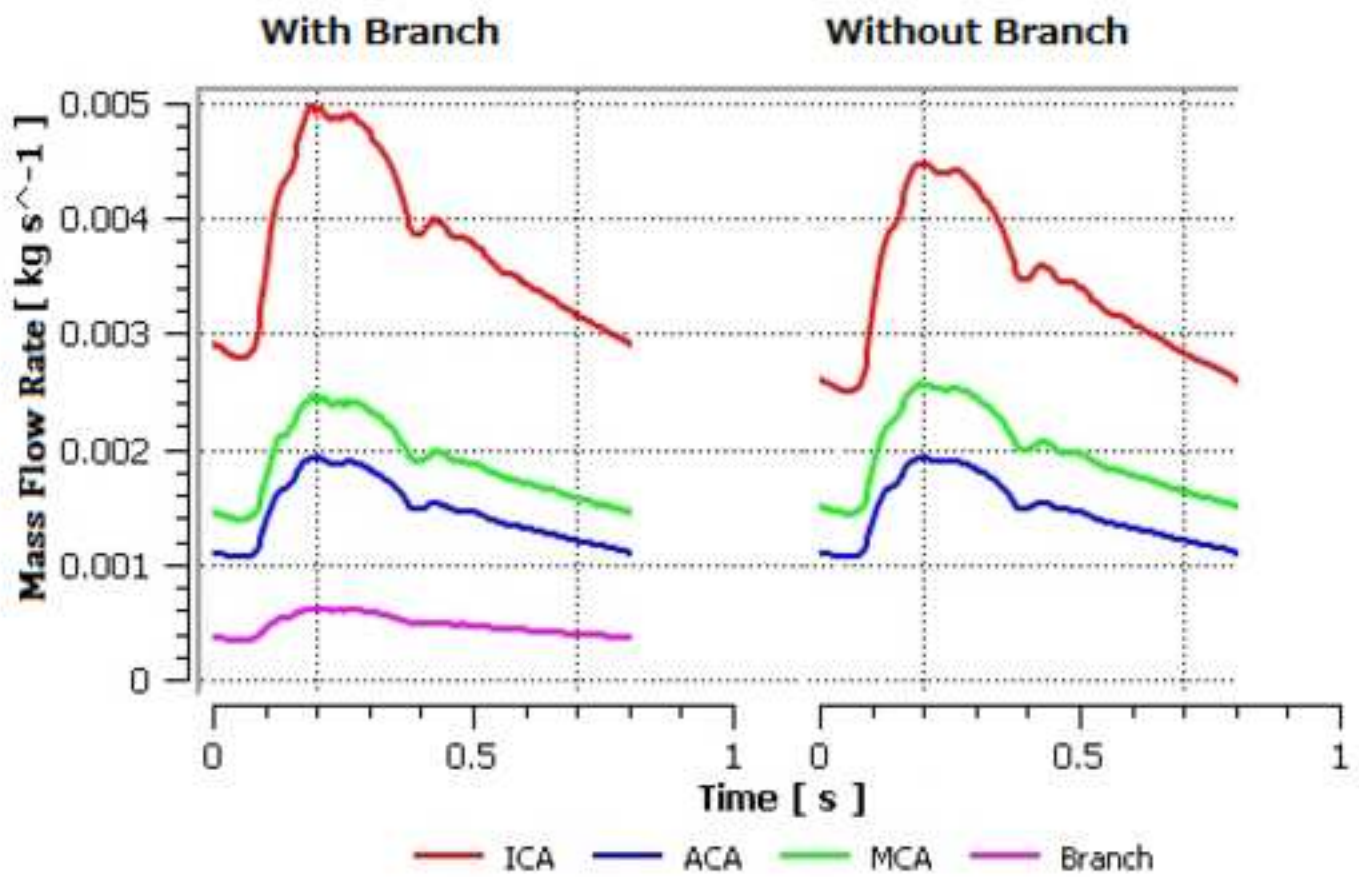


Figure(s)

[Click here to download high resolution image](#)

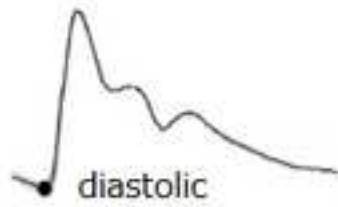


Figure(s)  
[Click here to download high resolution image](#)

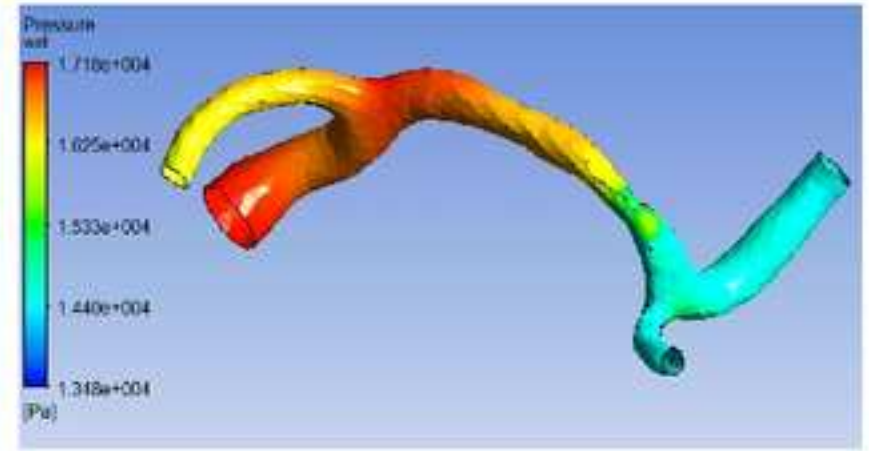
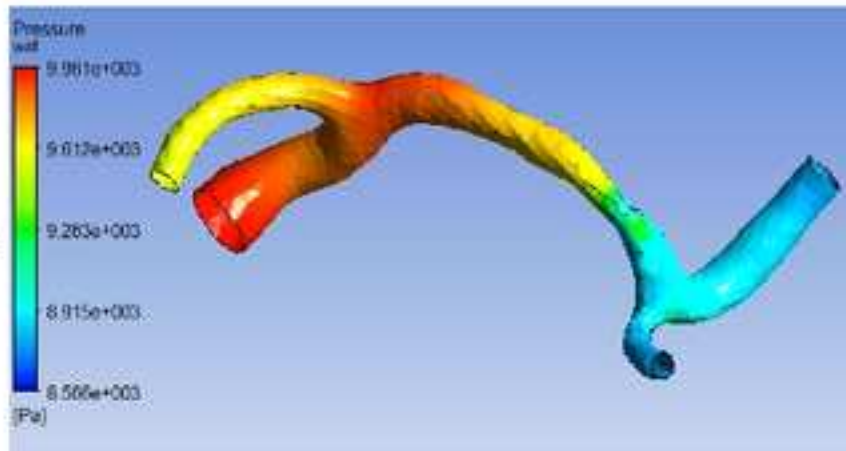


Figure(s)

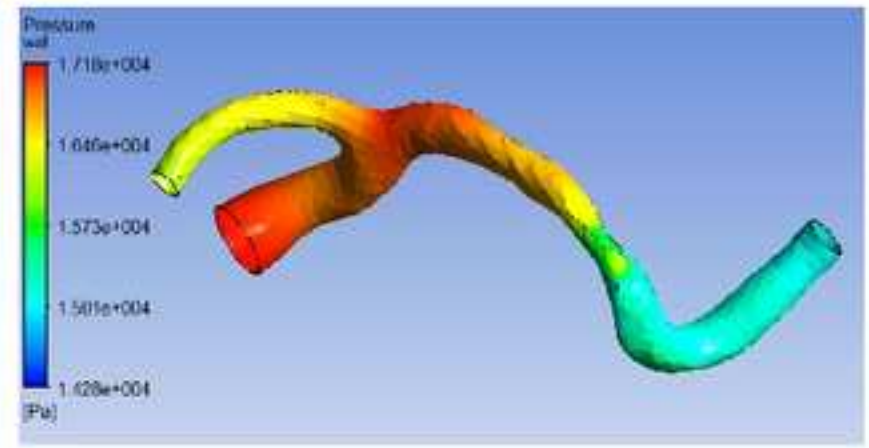
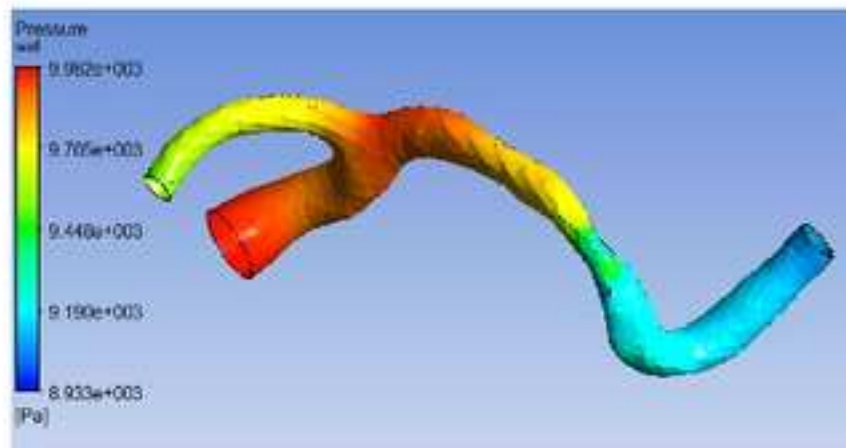
[Click here to download high resolution image](#)



**with  
branch**



**without  
branch**



Figure(s)  
[Click here to download high resolution image](#)

